

mosquitoes collected as immatures from known areas of WEE viral activity in order to provide further evidence for vertical transmission of WEE virus in nature. Finally, consideration should be given to factors that may influence the efficiency of vertical transmission of WEE virus in mosquitoes. For example, the temperature and salinity of the aquatic environment in which immature mosquitoes develop may influence the efficiency of vertical transmission.

REFERENCES AND NOTES

1. W. C. Reeves, *Epidemiology and Control of Mosquito-Borne Arboviruses in California, 1943-1987* (California Mosquito and Vector Control Association, Sacramento, CA, 1990).
2. W. K. Reisen and T. P. Monath, in *The Arboviruses: Epidemiology and Ecology*, T. P. Monath, Ed. (CRC Press, Boca Raton, FL, 1988), vol. 5, pp. 89-138.
3. B. F. Eldridge, G. C. Lanzaro, G. L. Campbell, W. C. Reeves, J. L. Hardy, *J. Med. Entomol.* **28**, 645 (1991).
4. Mosquito pools were assayed for virus according to the method described by G. L. Campbell, B. F. Eldridge, W. C. Reeves, and J. L. Hardy [*Am. J. Trop. Med. Hyg.* **44**, 244 (1991)] with minor modifications. Duplicate monolayer cultures of Vero cells were inoculated with material from each mosquito pool and then overlaid with a nutrient medium containing 1% Oxoid agar (Difco Laboratories, Detroit, MI). The duplicate cell cultures were incubated at 36°C in a humidified atmosphere of 5% CO₂ in air for 3 days, at which time a second overlay containing 1% Noble agar (Difco Laboratories, Detroit, MI) and neutral red (10 µg/ml) was applied to one of the duplicate cell cultures. Incubation of the duplicate cell cultures was continued for seven more days, and the culture that received the second overlay was examined daily for plaque formation. If plaques were observed, then virus was harvested from the duplicate cell culture and stored at -80°C.
5. Neutralization tests were done according to the method described by H. S. Lindsey, C. H. Calisher, and J. H. Mathews [*J. Clin. Microbiol.* **4**, 503 (1976)] with minor modifications. Tests were done in six-well plastic plates containing monolayer cultures of Vero cells. Antibody preparations included hyperimmune mouse ascitic fluids prepared to each of five members of the WEE serocomplex and one member of the EEE serocomplex (11). All antibody preparations were heat-inactivated (56°C for 30 min) and then serially diluted twofold (starting at 1:20) in a diluent containing 0.75% bovine albumin (v/v) and 8% fresh frozen human serum (v/v) on the day of the tests. All viruses were tested on the same day. Endpoint titers of the antibody preparations were expressed as the reciprocal of the highest dilution that inhibited 80% or more of a viral challenge of 50 to 100 plaque-forming units.
6. B. H. Kay, *Aust. J. Exp. Biol. Med. Sci.* **60**, 339 (1982).
7. J. R. O'venden and R. J. Mahon, *J. Med. Entomol.* **21**, 292 (1984).
8. R. O. Hayes *et al.*, *Am. J. Hyg.* **75**, 183 (1962).
9. R. W. Chamberlain and W. D. Sudia, *Annu. Rev. Entomol.* **6**, 371 (1961); P. B. Stones, cited in L. Rosen, *Am. J. Trop. Med. Hyg.* **37**, 69S (1987).
10. J. L. Hardy, *Am. J. Trop. Med. Hyg.* **37**, 18S (1987).
11. Hyperimmune mouse ascitic fluid to the BFS-1703 strain of WEE virus and to the DAV-3340 field isolate were prepared according to the method described by E. S. Tikasingh, L. Spence, and W. G. Downs [*Am. J. Trop. Med. Hyg.* **15**, 219 (1966)].
12. Highlands J virus (strain B-230), Fort Morgan virus (strain CM4-146), Sindbis virus (strain EgAr 339),

the Fleming strain of WEE virus, EEE virus (strain NJ/60), and the corresponding hyperimmune mouse ascitic fluids were provided by N. Karabatsos (Division of Vector-Borne Infectious Diseases, Centers for Disease Control and Prevention, Fort Collins, CO). We thank R. Chiles of the University of California, Berkeley, for technical

assistance in the laboratory studies. Supported by grants AI-26154 and AI-03028 from the National Institute of Allergy and Infectious Diseases and a grant from the San Mateo County Mosquito Abatement District (Burlingame, CA).

16 August 1993; accepted 22 November 1993

Lack of Acidification in *Mycobacterium* Phagosomes Produced by Exclusion of the Vesicular Proton-ATPase

Sheila Sturgill-Koszycki, Paul H. Schlesinger, Prasanta Chakraborty, Pryce L. Haddix, Helen L. Collins, Agnes K. Fok, Richard D. Allen, Stephen L. Gluck, John Heuser, David G. Russell*

The success of *Mycobacterium* species as pathogens depends on their ability to maintain an infection inside the phagocytic vacuole of the macrophage. Although the bacteria are reported to modulate maturation of their intracellular vacuoles, the nature of such modifications is unknown. In this study, vacuoles formed around *Mycobacterium avium* failed to acidify below pH 6.3 to 6.5. Immunoelectron microscopy of infected macrophages and immunoblotting of isolated phagosomes showed that *Mycobacterium* vacuoles acquire the lysosomal membrane protein LAMP-1, but not the vesicular proton-adenosine triphosphatase (ATPase) responsible for phagosomal acidification. This suggests either a selective inhibition of fusion with proton-ATPase-containing vesicles or a rapid removal of the complex from *Mycobacterium* phagosomes.

Mycobacterium spp. are the causative agents of a spectrum of human diseases. Both *Mycobacterium tuberculosis* and *M. avium* have attracted attention through their increasing prevalence, particularly among immunocompromised individuals, and their resistance to current chemotherapeutic regimens (1, 2). The key to *Mycobacterium*'s success lies in its interaction with the host macrophage and its strategies for survival inside this potentially hostile cell. Much attention has been directed toward the nature of *Mycobacterium*-containing vacuoles, and although the literature concerning the accessibility of these compartments to freshly endocytosed material is contradictory (3), a significant number of laboratories have reported failure of electron-dense colloids to enter previously formed *Mycobacterium* vacuoles (4). In addition, recent analysis of *M. avium*-containing vacuoles revealed a correlation between inhibition of lysosomal fusion and survival of bacteria in macrophages from *bcg*^r and *bcg*^s mice (5). The restricted

fusigenicity of the mycobacterial vacuole may extend beyond limiting access of lysosomal hydrolases to the bacilli, and both Gordon (6), indirectly through the use of acridine orange, and Crowle (7), using the weak base DAMP, had reported that the bacterial vacuole was relatively less acidic than neighboring lysosomes.

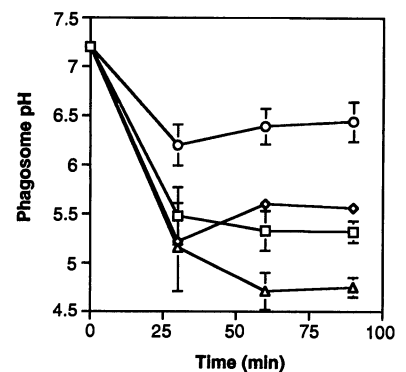


Fig. 1. Measurement of phagosomal pH. Graph illustrates the pH of phagosomes formed around human IgG-coated latex beads, *L. mexicana* tissue-culture amastigotes, zymosan, and *M. avium* (9). The pH of IgG-beads (◇), zymosan (△), and *Leishmania* phagosomes (□) rapidly decreased below 5.5 within the first 30 min after uptake. In contrast, the pH of *M. avium* phagosomes (○) decreased to about 6.3 before equilibrating to 6.5. The pH of the phagosomes was measured by spectrofluorimetry of NHS-carboxyfluorescein-labeled particles (9).

S. Sturgill-Koszycki, P. Chakraborty, P. L. Haddix, H. L. Collins, D. G. Russell, Department of Molecular Microbiology, Washington University Medical Center, St. Louis, MO 63110.
P. H. Schlesinger and J. Heuser, Department of Cell Biology and Physiology, Washington University Medical Center, St. Louis, MO 63110.
S. L. Gluck, Department of Medicine, Washington University Medical Center, St. Louis, MO 63110.
A. K. Fok and R. D. Allen, Department of Microbiology, University of Hawaii, Honolulu, HI 96822.

*To whom correspondence should be addressed.

Internalization of *Mycobacterium* species by macrophages is mediated by known phagocytic receptors (8). To determine the extent to which the bacterium modulates the function of the vacuole after internalization, we measured the pH of phagosomes formed around *M. avium*, *Leishmania mexicana*, immunoglobulin G (IgG)-coated latex beads, and zymosan. These particles were fluoresceinated and exhibited a pH-sensitive fluorescence-emission profile (9). IgG-beads are inert particles internalized through a defined receptor, FcγRII, and the parasitophorous vacuoles formed by the protozoan pathogen *Leishmania* are known to be acidic and fuse directly with the macrophage's endocytic network (10, 11). The IgG-coated beads, zymosan, and *Leish-*

mania were internalized into phagosomes that acidified to pH 5.5 or below (Fig. 1). In contrast, phagosomes containing *M. avium* equilibrated to pH 6.3 to 6.5. The results confirm and quantify previous proposals (6, 7) that *Mycobacterium* phagosomes are unable to fully acidify. The pK of N-hydroxysuccinimide (NHS)-carboxyfluorescein (5.4 to 5.8) is well suited to determination of vacuolar pH; however, the limited acidification that we report for the *M. avium*-containing phagosomes is likely a minimum pH value. Some limited acidification may occur in *M. avium* phagosomes as a function of other vesicular transporters, such as the Na⁺/K⁺ATPase, the Na⁺/H⁺exchanger, or the chloride channel, or as a result of the metabolic activity of *Mycobacterium* itself. Maintenance of the phagosomal pH around 6.5 would severely restrict lysosomal hydrolase activity, enhancing the intracellular survival capacity of the bacilli.

Immunoelectron microscopy of *M. avium*- and *M. tuberculosis*-containing phagosomes (12) (Fig. 2) revealed the presence of the lysosomal-endosomal marker LAMP-1 (13), suggesting that some mixing with components of the macrophage's endosomal network had occurred. LAMP-1-Igp 1 has been used as a correlate of

lysosomal fusion in studies on *Toxoplasma* host-cell invasion (14). The density of LAMP-1 signal in the mycobacterial vacuoles is comparable to that of the IgG-bead and *Leishmania*-containing vacuoles (Fig. 2). An antibody to the 116-kD accessory subunit from the proton-ATPase of *Dictyostelium* (15), which reacted with its 110-kD mammalian homolog, labeled the membrane of both the IgG-bead and *Leishmania* vacuoles yet failed to label the *Mycobacterium* phagosomes (Fig. 2), providing preliminary evidence that the lack of acidification in these vacuoles could correlate with an absence of the proton-ATPase.

To determine whether acidification of *Mycobacterium* phagosomes is limited by exclusion of the proton-ATPase, we isolated *M. avium*-containing vacuoles for analysis (16). Platinum replicas were made of the cytoplasmic faces of *Leishmania*- and *Mycobacterium*-containing phagosomes (Fig. 3). There was a marked difference in the protein complexes associated with the cytoplasmic membrane surface. This face of the *Leishmania* vacuoles was studded with 15-nm "pegs," whereas *Mycobacterium* vacuoles were smooth. These "pegs" bear a marked resemblance to the proton-ATPase complexes on the contractile vacuoles of the slime mold *Dictyostelium* (17), also shown in

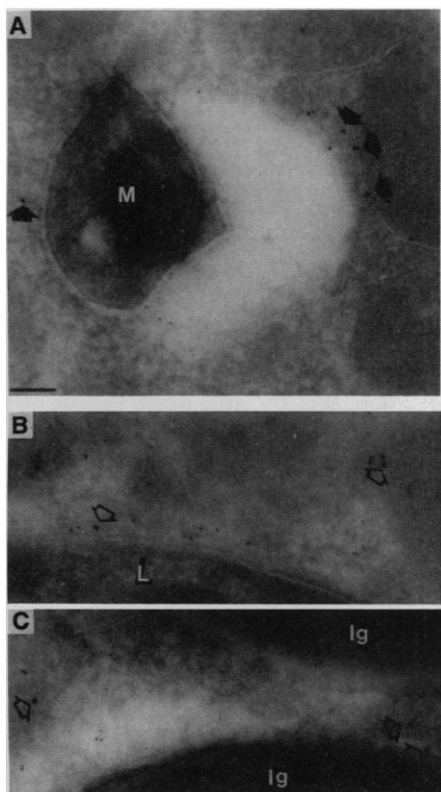


Fig. 2. Immunoelectron microscopy of *M. avium* in bone marrow-derived murine macrophages. Phagosomes were labeled for 60 min in situ with antibodies to LAMP-1 (anti-LAMP-1) (ID4B-5-nm gold anti-rat IgG) and to the 110-kD proton-ATPase accessory subunit (anti-110) (N2-12-nm gold anti-mouse IgG). (A) The *M. avium* (labeled M) phagosome binds anti-LAMP-1 but does not react with anti-110, although anti-110 labels the membranes surrounding dense lysosomal bodies in the vicinity of the mycobacterial vacuole (arrowed). In contrast, the phagosomes containing *Leishmania* (labeled L) (B) and IgG-beads (labeled Ig) (C) react with both anti-LAMP-1 and anti-110 (arrowed). Comparable amounts of LAMP-1 labeling were observed in all three phagosome preparations. Material was processed as described (10). Bar, 0.1 μm.

Fig. 3. Electron microscopy of isolated *M. avium*-containing phagosomes and vacuoles. (A and B) Transmission electron microscopy of isolated phagosomes released from bone marrow-derived macrophages 60 min after internalization. (C to G) Freeze-etch electron microscopy of isolated phagosomes and vacuoles revealing the cytoplasmic face of the particle-containing vesicles. (C) Low-magnification view of an *L. mexicana*-containing phagosome isolated 60 min after internalization. The surface of the phagosome is studded with "pegs," or protein complexes. (D) Low-magnification view of an *M. avium*-containing vacuole isolated 4 days after infection. This vacuole is completely smooth, as were vacuoles isolated at 30 min, 2 hours, and 4 days. (E to G) High-magnification micrographs of smooth *M. avium* phagosome surface (E) as compared to the "pegs" on the *Leishmania* phagosome (F) and the proton-ATPases on the contractile vacuole of *Dictyostelium* (G) (17). Phagocytic vacuoles were isolated as described (16, 25). Bar, 1 μm (A to D) or 0.1 μm (E to G).

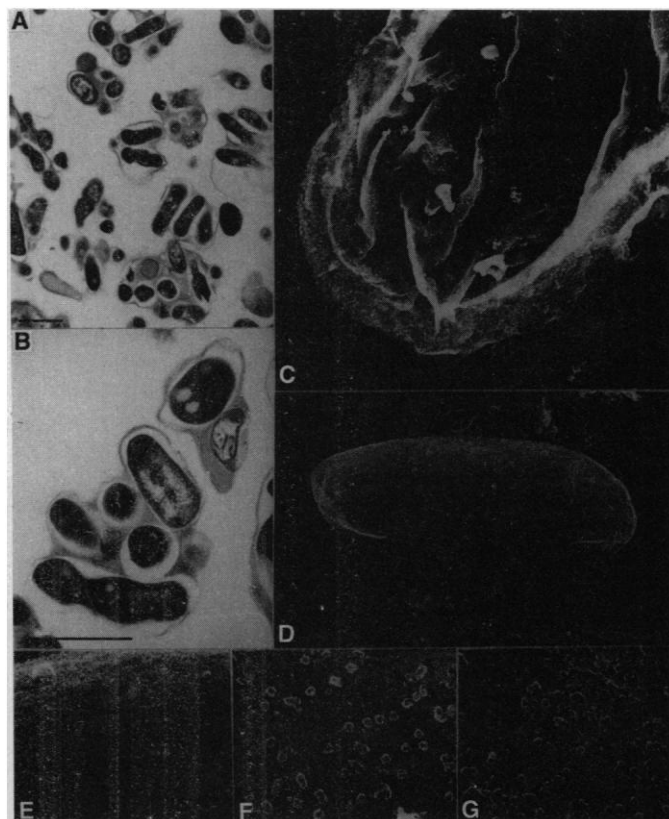


Fig. 3. To confirm the identity of the "peg" structures as proton-ATPase molecules and to determine which proton-ATPase subunits were absent from *Mycobacterium* vacuoles, we immunoblotted equivalent amounts of proteins from isolated phagosomes and probed the proteins with antibodies to lysosomal constituents (Fig. 4). The antibodies were specific for LAMP-1 (13), the E (31 kD) and B (56 kD) subunits of the mammalian vesicular proton-ATPase, and the 110-kD accessory protein (18). LAMP-1 was present in comparable amounts on all types of vacuoles, including *M. avium*-containing vacuoles. In contrast, the E subunit was present in the *Leishmania* vacuoles and the IgG-bead phagosomes, which also contained the B subunit. Both these subunits were absent from *M. avium* vacuoles. As neither the E nor B subunits are intrinsic membrane proteins, their absence from the *M. avium* vacuoles could be due to dissociation of the hydrophilic "heads" of the proton-ATPase complex or failure of proton-ATPase-containing vesicles to fuse with, or be retained by, the *Mycobacterium* vacuoles. However, absence of the 110-kD accessory protein, which is an integral membrane protein (19, 20), from the *M. avium* vacuoles indicates that the bacterium inhibits incorporation or retention of intact proton-ATPases by the phagosome, rather than dissociating the cytoplasmic proton-ATPase subunits. These data do not differentiate inhibition of fusion with proton-ATPase-carrying vesicles from the rapid removal of proton-ATPase complexes from the phagosomes.

Much of the current knowledge on the maturation of phagosomes is inferred from studies on endosomes rather than from direct experimentation. During endocytosis, vacuoles acidify rapidly, indicating that the proton-ATPase is either delivered early to the endosome (21) or is internalized with the plasmalemma (22). Our observations with phagosomes indicate that the proton-ATPase accumulates shortly after internalization, yet its delivery or retention in mycobacterial vacuoles is independent of the accumulation of LAMP-1. The simplest explanation for our results is that *Mycobac-*

terium selectively inhibits fusion of its vacuole with proton-ATPase-positive vesicles, while actively fusing with LAMP-1-carrying vesicles. The ability of *Mycobacterium* species to inhibit fusion of their vacuoles with lysosomal compartments may reflect a related mechanism. This interpretation requires that the vesicles responsible for delivery of endosomal constituents are heterogeneous, facilitating their differential accumulation. The vehicle for delivery of proton-ATPase complexes to the phagosome is still not defined, and *Mycobacterium* may prove useful in helping to analyze this aspect of phagosomal maturation.

In an established mycobacterial infection, the mycobacterial lipodiglycan, lipoarabinomannan (LAM) (23), is secreted into both *M. avium*- and *M. tuberculosis*-containing vacuoles and subsequently transferred into dense lysosome-like vesicles (12). Even in 14-day infections the immunocytochemical density of LAMP-1, as well as the integrity of the vacuolar membrane, is maintained around the *Mycobacterium*. So, despite the loss of membrane through the pinching-off of LAM-containing vesicles and the formation of fresh, discrete vacuoles as the bacilli divide, both the vacuolar membrane and LAMP-1 density are sustained. These data indicate that the mycobacterial vacuole cannot be disconnected from all intracellular trafficking pathways and must be replenished by fusion with intracellular vesicles. Nevertheless, the absence of proton-ATPases is maintained, and therefore stable incorporation of membrane proteins into the *Mycobacterium* vacuole must retain selectivity. Because the compartments show limited fusion with plasmalemma-derived endosomal membrane (12), the *Mycobacterium* vacuoles must acquire LAMP-1 through fusion with vesicles originating elsewhere in the cell. We suggest that the freshly synthesized components budding from the trans-Golgi network could provide an alternative source of host membrane and proteins.

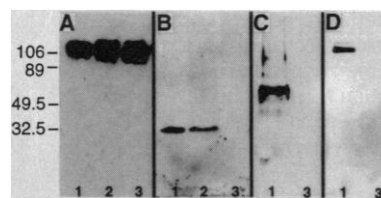
Mycobacterium species are persistent infective agents that are highly refractory both to chemotherapy and the microbicidal

responses of activated macrophages. The ability of these bacilli to modulate their intracellular compartments is essential to the organism's success. Preliminary evidence that the relatively high pH of the mycobacterial vacuole is important in reducing the potency of cytokine-induced bacteriostatic responses in host macrophages has recently been reported (24). The data described here have implications for our understanding of both the pathogenesis of *Mycobacterium* infections and the phagosome-maturation pathway.

REFERENCES AND NOTES

1. Y. Zhang, B. Heym, B. Allen, D. Young, S. Cole, *Nature* 358, 591 (1992).
2. B. R. Bloom *et al.*, *ibid.*, p. 538.
3. U. Steinhoff, J. R. Golecki, J. Kazda, S. H. E. Kaufmann, *Infect. Immun.* 57, 1008 (1989).
4. C. Frehel, C. C. de Chastellier, T. Lang, N. Rastogi, *ibid.* 52, 252 (1986); C. Frehel and N. Rastogi, *ibid.* 55, 2916 (1987); P. D. Hart and M. R. Young, *J. Exp. Med.* 174, 881 (1991); L. D. Sibley, S. G. Franzblau, J. L. Krahenbuhl, *Infect. Immun.* 55, 680 (1987); N. Rastogi, M. Bachelet, J. P. Carvalho de Souza, *Microbiol. Immunol.* 89, 273 (1992).
5. C. de Chastellier, C. Frehel, C. Offredo, E. Skamene, *Infect. Immun.* 61, 3775 (1993).
6. A. H. Gordon, P. D'arcy Hart, M. R. Young, *Nature* 286, 79 (1980).
7. A. J. Crowe, R. Dahl, E. Ross, M. H. May, *Infect. Immun.* 59, 1823 (1991).
8. L. S. Schlesinger, C. G. Bellinger-Kawahara, N. R. Payne, M. A. Horwitz, *J. Immunol.* 144, 2771 (1990); L. S. Schlesinger and M. A. Horwitz, *ibid.* 147, 1983 (1991).
9. L. G. Eisenberg, W. Goldman, P. H. Schlesinger, *J. Exp. Med.* 177, 1605 (1993). Particles were labeled with NHS-carboxyfluorescein (250 µg/ml; Boehringer Mannheim) in bicarbonate saline (pH 7.6) on ice for 20 min and washed in three to four changes of Dulbecco's minimum essential medium with 10% fetal calf serum and 5% horse serum. This did not affect the viability of either *L. mexicana* (MYNC/BZ/62/M379) or *M. avium* (strain 101). Monolayers of murine bone-marrow macrophages were established on 1 by 2.5 cm glass slides, and particles were added on ice at ratios to produce four to eight particles bound per cell (*Leishmania*, 10:1; IgG-beads, 10:1; and *M. avium*, 25:1). After settling on ice for 10 min, the cells were left at room temperature for 5 min, washed by immersion, and placed in medium prewarmed to 37°C. Calibration for each fluorescent particle was conducted in situ. All fluorescent determinations were done with an Aminco SPF500 spectrofluorimeter thermostat regulated to 37°C. The relative fluorescence values were measured and averaged over 3 s at an emission wavelength of 524 nm and excitation at both 450 and 497 nm. The fraction of particles accessible to the cell surface was controlled for and found to be negligible by measurement of the response to alterations in the pH of the external buffer.
10. D. G. Russell, S. Xu, P. Chakraborty, *J. Cell. Sci.* 103, 1193 (1992).
11. J. C. Antoine, E. Prina, C. Jouanne, P. Bongrand, *Infect. Immun.* 58, 779 (1990).
12. S. Xu *et al.*, unpublished results.
13. J. W. Chen, G. L. Chen, M. P. D'Souza, T. L. Murphy, J. T. August, *Biochem. Soc. Symp.* 51, 97 (1986).
14. K. A. Joiner, S. A. Fuhrman, H. M. Miettinen, L. H. Kasper, I. Mellman, *Science* 249, 641 (1990).
15. A. K. Fok, M. Clarke, S. Ma, R. D. Allen, *J. Cell. Sci.*, in press.
16. P. Chakraborty, S. Sturgill-Koszycki, D. G. Russell, unpublished results. *Mycobacterium avium*-vacuoles were isolated by lysing of infected mac-

Fig. 4. Protein immunoblot analysis of isolated *M. avium*-, *Leishmania*-, and IgG-bead-containing vacuoles revealing the absence of proton-ATPase subunits from *M. avium* vacuoles. Gel panels were probed with (A) rat monoclonal antibody (mAb) to LAMP-1, (B) a mouse mAb to the 31-kD E subunit, (C) an affinity-purified rabbit polyclonal antibody to the 56-kD B subunit, and (D) mouse mAb to the 110-kD accessory protein. SDS-polyacrylamide gel electrophoresis (PAGE) gels (10%) were run with IgG-bead phagosomes (60 min, lane 1), *Leishmania* phagosomes (60 min, lane 2), and *M. avium* phagosomes (60 min, lane 3). *Leishmania* phagosomes were omitted from (C) and (D) because of antibody reactivity with *Leishmania* proton-ATPases. Total homogenates of *M. avium*-infected macrophages reacted with all antibodies. Phagosomes were prepared as described (16, 25). Molecular size markers are indicated on the left (in kilodaltons).



rophages on ice in a stainless steel homogenizer into 20 mM Hepes, 0.5 mM EGTA, 250 mM sucrose, and 0.5% gelatin (pH 7.0) with 10 μ M TLCK and leupeptin. Unbroken cells and nuclei were sedimented by centrifugation and the supernatant passed through a 3- μ m pore Nucleopore filter. The flow-through was centrifuged through a 12% sucrose cushion at 1700g for 45 min and collected at the tube base. *Leishmania* phagosomes were isolated into the same lysis mixture by disruption with ~30 passages through 50 mm of 0.6-mm bore plastic tubing. After a low-speed spin to sediment large debris, the supernatant was loaded onto a discontinuous sucrose step gradient (60%, 40%, 20%, and homogenate) and centrifuged at 1700g for 25 min. The phagosomes were harvested from the 40 to 60% interface. The purity of these and subsequent phagosome prep-

arations was monitored by electron microscopy.

17. J. Heuser, Q. Zhu, M. Clarke, *J. Cell Biol.* **121**, 1311 (1993).
18. R. D. Nelson *et al.*, *Proc. Natl. Acad. Sci. U.S.A.* **89**, 3541 (1992).
19. N. Nelson, *Curr. Opin. Cell Biol.* **4**, 654 (1992).
20. M. S. Perin, V. A. Fried, D. K. Stone, X. S. Xie, T. C. Suedhof, *J. Biol. Chem.* **266**, 3877 (1991).
21. I. Mellman, *J. Exp. Biol.* **172**, 39 (1992).
22. N. Marquez-Sterling *et al.*, *Eur. J. Cell Biol.* **56**, 19 (1991).
23. J. Chan *et al.*, *Infect. Immun.* **59**, 1755 (1991).
24. R. Appleberg and I. M. Orme, *Immunology* **80**, 352 (1993).
25. The IgG-beads were prepared by reaction of tosylactivated, iron-containing, 2.8- μ m latex beads (Dynal) with human IgG. The IgG-bead phagosomes were isolated by lysis of macro-

phages in homogenization buffer by passage through narrow-gauge tubing (16) and washed (four times) after magnetic selection in a Dynal MPC apparatus. SDS-PAGE gels were run with phagosome preparations normalized to equivalent amounts of LAMP-1 protein. Nitrocellulose blots were probed with primary antibodies and species-specific, horseradish peroxidase-conjugated secondary antibodies (Jackson ImmunoResearch Laboratories). The blots were developed by enhanced chemiluminescence (Amersham).

26. Supported by USPHS grants AI26889 and AI34207 (to D.G.R.) and by USPHS award AR42370 (to P.H.S.). D.G.R. would like to thank N. Connell, B. Bloom, I. Orme, and P. Brennan for their introduction to *Mycobacterium*.

23 June 1993; accepted 18 November 1993

Magnetic Resonance Microscopy of Embryonic Cell Lineages and Movements

Russell E. Jacobs* and Scott E. Fraser

Key events in vertebrate embryogenesis are difficult to observe in many species. High-resolution magnetic resonance imaging was used to follow cell movements and lineages in developing frog embryos. A single cell was injected at the 16-cell stage with a contrast agent, based on the gadolinium chelate gadolinium-diethylenetriamine pentaacetic acid-dextran. The labeled progeny cells could be followed uniquely in three-dimensional magnetic resonance images, acquired from the embryo over several days. The results show that external ectodermal and internal mesodermal tissues extend at different rates during amphibian gastrulation and neurulation.

The analysis of cell lineages and cell movements is central to an understanding of the processes by which an adult vertebrate develops. The opacity and large number of indistinguishable cells in the vertebrate embryo prohibit analysis by direct observation (1). The tracing of cell movements and lineages requires some means to render a cell and its progeny unique. Individual precursors have been labeled with membrane-impermeable enzymes (2) or fluorescent dyes (3), or infected with a retroviral agent (4). With few exceptions (5), subsequent observation of the progeny requires fixed, sectioned, and stained specimens. This processing prohibits the direct observation of ongoing developmental events; instead, they must be inferred by comparison of results obtained from different embryos fixed at different stages.

This limitation is especially critical in studies of early morphogenetic events in the vertebrate embryo, such as gastrulation in amphibians. Although *Xenopus laevis* has served as the central system for analyses of vertebrate gastrulation movements and the cell interactions that they bring about, most of the movements of cells cannot be followed in the intact embryo because they take place largely

within its interior. Thus, analyses of these processes in *X. laevis* have relied on time-lapse cinematography of surface cell movements, histological examination of fixed specimens, and explantation techniques (6). The results of these studies have demonstrated the coupling of the convergence of cells toward the dorsal midline with the extension of the embryonic axis (convergent extension) brought about by changes in cell shape and relative positioning (radial and mediolateral intercalation). Short-range intercalary movements can bring about large-scale tissue movements. For example, a simple mediolateral intercalation of each cell moving between its neighbors toward the midline results in a doubling of the tissue length (extension) and halving of the tissue width (convergence). Explant cultures show such convergence-extension movements during gastrulation, both in the cells that remain on the surface of the embryo (noninvoluting marginal zone) and in those that involute to form the expanding archenteron (involuting marginal zone).

To observe ongoing developmental events in living frog embryos, we used high-resolution magnetic resonance imaging (MRI). With MRI, three-dimensional (3D) images of the developing embryo may be obtained on a time scale faster than the cell division time and analyzed forward or backward in time to reconstruct fully cell divisions and cell movements. The MRI

technique is a qualitatively different method of visualization than the light microscopy used in previous lineage studies. In this method, the recorded signal arises from the hydrogen nuclear spin of water molecules. Spatial localization of the nuclear magnetic resonance (NMR) signal is made possible by superimposing various magnetic field gradients on the usual static magnetic field (7). The use of a set of three orthogonal gradients allows the NMR signal to be parsed into a matrix of intensities, one for each volume element (voxel), yielding the 3D magnetic resonance image. Contrast in the magnetic resonance image arises from voxel-to-voxel variations in the water concentration and local environment. Variations in the local environment (for example, proximity to a paramagnetic center) and state (for example, mobile versus immobile) of the water modulate the NMR relaxation times T_1 and T_2 (8). We use an imaging protocol that yields an image in which the intensity is a monotonic function of the relaxation rate ($1/T_1$) (9).

To perform cell lineage analyses with MRI, an MRI lineage tracer is required that must (i) induce a local signal that is characteristically different from that of the rest of the sample, (ii) be physiologically inert, and (iii) remain within the originally labeled cell and its progeny. MRI contrast enhancement agents based on gadolinium have the needed effect on the MRI water signal, increasing the relaxation rates of nearby nuclear spins to provide contrast not naturally found in the specimen (10). We used an MRI contrast agent that is a covalent conjugate of dextran with diethylenetriamine pentaacetic acid (DTPA) to which Gd^{3+} has been chelated (11). The high-affinity chelator DTPA protects living systems from the toxic effects of Gd^{3+} (12). We used twice as much chelator as Gd^{3+} to ensure that a minimal amount of free Gd^{3+} was present. The dextran is membrane-impermeant and too large to pass from cell to cell through gap junctions, thereby limiting the contrast agent to the injected cells and their descendants. Because this tracer is

Division of Biology, Beckman Institute (139-74), California Institute of Technology, Pasadena, CA 91125.

*To whom correspondence should be addressed.